

Role of Basic Residues of the Autolysis Loop in the Catalytic Function of Factor Xa[†]

Chandrashekhara Manithody, Likui Yang, and Alireza R. Rezaie*

Edward A. Doisy Department of Biochemistry and Molecular Biology, Saint Louis University School of Medicine, Saint Louis, Missouri 63104

Received January 10, 2002; Revised Manuscript Received March 4, 2002

ABSTRACT: The autolysis loop of factor Xa (fXa) has four basic residues (Arg¹⁴³, Lys¹⁴⁷, Arg¹⁵⁰, and Arg¹⁵⁴) whose contribution to protease specificity of fXa has not been examined. Here, we substituted these basic residues individually with Ala in the fX cDNA and expressed them in mammalian cells using a novel expression/purification vector system. Following purification to homogeneity and activation by the factor X activator from Russell viper venom, the mutants were characterized with respect to their ability to assemble into the prothrombinase complex to activate prothrombin and interact with target plasma fXa inhibitors, tissue factor pathway inhibitor (TFPI) and antithrombin. We show that all mutants interacted with factor Va with normal affinities and exhibited wild-type-like prothrombinase activities toward prothrombin. Lys¹⁴⁷ and Arg¹⁵⁴ mutants were inhibited by TFPI ~2-fold slower than wild type; however, both Arg¹⁴³ and Arg¹⁵⁰ mutants were inhibited normally by the inhibitor. The reactivities of Arg¹⁴³ and Lys¹⁴⁷ mutants were improved ~2-fold with antithrombin in the absence but not in the presence of heparin cofactors. On the other hand, the pentasaccharide-catalyzed reactivity of antithrombin with the Arg¹⁵⁰ mutant was impaired by an order of magnitude. These results suggest that Arg¹⁵⁰ of the autolysis loop may specifically interact with the activated conformation of antithrombin.

Factor Xa (fXa)¹ is a vitamin K-dependent serine protease in plasma that is responsible for generation of thrombin from prothrombin in the coagulation cascade (1–4). It circulates in plasma as a light- and heavy-chain molecule held together by a disulfide bond (5). The N-terminal light chain contains the noncatalytic Gla and two epidermal growth factor-like domains, while the C-terminal heavy chain contains the trypsin-like catalytic domain of the molecule (6). Two different types of physiological inhibitors, the tissue factor pathway inhibitor (TFPI) and antithrombin, regulate the proteolytic activity of fXa in plasma. TFPI is a multidomain Kunitz-type inhibitor that regulates coagulation by the fXa-dependent inhibition of the factor VIIa–tissue factor complex during the initial stages of the clotting cascade (7). It functions by binding to the active site pocket of fXa by the second Kunitz domain, and thereafter binding tightly to the active site of the factor VIIa–tissue factor complex via the first Kunitz domain, thereby rendering both proteases inactive in a quaternary complex (7, 8). Antithrombin, on the other hand, is a serine protease inhibitor (serpin) that regulates

the proteolytic activity of fXa and other coagulation proteases by binding to the active sites through an exposed reactive center loop, and undergoing a conformational change which traps the enzymes in inactive, stable complexes (9, 10).

Except for the high-affinity interaction of fXa with TFPI which is independent of a cofactor, fXa requires a cofactor to effectively activate prothrombin or react with antithrombin under physiological conditions. Thus, complex formation of fXa with factor Va in the prothrombinase complex promotes the catalytic efficiency of the protease by 4–5 orders of magnitude (3, 4). Similarly, in reaction with antithrombin, full-length heparins, resembling the anticoagulant active glycosaminoglycans found in vivo (11), function as cofactors to accelerate the rate of fXa inhibition by the serpin by 4–5 orders of magnitude under physiological levels of Ca²⁺ (12, 13). Such dramatic enhancement in the catalytic efficiency of fXa in these reactions is thought to arise from the ability of cofactors to either directly assemble the protease with its target molecules in ternary complexes (14, 15) and/or induce allosteric changes in the structure of these molecules, leading to exposure of new sites, “exosites”, near or remote from the catalytic pocket of the protease (16, 17) or the reactive site loop of the serpin (18, 19). By such mechanisms, both types of cofactors facilitate macromolecular complex assembly and productive interaction of the reacting residues in the enzyme–substrate or enzyme–inhibitor reactions. For instance, it is known that factor Va, by binding directly to both fXa and prothrombin (15), and heparin, by binding to both fXa and antithrombin (20), can mediate macromolecular complex assemblies leading to dramatic improvements in the rate of catalytic reactions. Moreover, factor Va in the

[†] The research discussed herein was supported by a grant awarded by the National Heart, Lung, and Blood Institute of the National Institutes of Health (Grant R01 HL 62565 to A.R.R.).

* Address correspondence to this author at the Department of Biochemistry and Molecular Biology, St. Louis University School of Medicine, 1402 S. Grand Blvd., St. Louis, MO 63104. Phone: (314) 577-8130, Fax: (314) 577-8156, E-mail: rezaiear@slu.edu.

¹ Abbreviations: fXa, activated factor X; pfXa, plasma-derived fXa; rfXa, recombinant fXa; PT, prothrombin time; R143A, K147A, R150A, and R154A, fXa derivatives in which Arg¹⁴³, Lys¹⁴⁷, Arg¹⁵⁰, and Arg¹⁵⁴ in the chymotrypsinogen numbering system (24) have been replaced with Ala; serpin, serine protease inhibitor; H₅, pentasaccharide; PEG, poly(ethylene glycol).

prothrombinase complex is reported to expose an exosite on fXa that is a specific recognition site for interaction with prothrombin (16, 17), and a unique pentasaccharide fragment of heparin is known to induce conformational changes in the structure of antithrombin that facilitate its efficient reaction with fXa (18, 19, 21). The molecular determinants of specificity on fXa that are responsible for these types of cofactor-mediated interactions with its physiological macromolecules have not been identified.

Structural data suggest that the catalytic domain of fXa, similar to those of other coagulation proteases, has several surface loops that surround the substrate-binding pocket of the enzyme (22, 23). Although these surface loops are generally conserved at homologous regions on the catalytic domain of all serine proteases, their lengths and amino acid compositions are, nonetheless, unique for each member of the family, suggesting that they may participate in determination of substrate and inhibitor specificity of these proteases. One of these surface loops consisting of residues 143–154 [chymotrypsinogen numbering (24)], referred to as the autolysis loop, is known to play a crucial role in determination of substrate and inhibitor specificity of thrombin (25) and activated protein C (26). This loop of fXa contains four basic residues, Arg¹⁴³, Lys¹⁴⁷, Arg¹⁵⁰, and Arg¹⁵⁴, whose contribution to protease specificity of fXa has not been studied. To understand the function of these residues in fXa, we substituted them individually with Ala in the factor X cDNA in four separate constructs and expressed the mutant zymogens in mammalian cells. Following activation by the factor X activator from Russell viper venom (RVV-X), the mutants were characterized with respect to their ability to assemble into the prothrombinase complex to activate prothrombin and interact with target plasma fXa inhibitors, tissue factor pathway inhibitor (TFPI) and antithrombin. The results indicate that basic residues of the autolysis loop are dispensable for the recognition specificity of fXa in its reaction with prothrombin in either the absence or the presence of factor Va on negatively charged phospholipid vesicles. The affinities of Arg¹⁴³ and Arg¹⁵⁰ mutants for binding TFPI were normal, and those of Lys¹⁴⁷ and Arg¹⁵⁴ mutants were impaired ~2-fold. In reaction with antithrombin, Arg¹⁴³ and Lys¹⁴⁷ mutants reacted with fXa with ~2-fold improved rate constants in the absence, but not in the presence, of heparin cofactors. On the other hand, the reactivity of the Arg¹⁵⁰ mutant was impaired by an order of magnitude in the presence of pentasaccharide which is known to allosterically activate the serpin. These results suggest that the basic residues of the autolysis loop play a crucial role in fXa recognition of native and activated conformations of antithrombin.

MATERIALS AND METHODS

Mutagenesis and Expression of Recombinant Proteins. We have prepared a novel expression/purification vector system for fX and its mutants in mammalian cells. Factor X is believed not to express efficiently in mammalian cells because it lacks a tri-basic recognition site for furin-like processing enzymes responsible for the cleavage of the prepropeptides of coagulation zymogens (27, 28). Unlike other vitamin K-dependent coagulation zymogens, a single basic residue (Arg⁴⁰) constitutes the P1 site of this recognition sequence in the light chain of fX (29). To facilitate efficient

expression, we introduced two additional basic residues to this site of fX cDNA by replacing Val³⁸ and Thr³⁹ at the P3 and P2 positions, with an Arg and a Lys, respectively (Figure 1). Moreover, to facilitate the purification of fX derivatives, we replaced the first 12 residues of the activation peptide of fX [residues 183–194 in fX numbering (29)] on the heavy chain with the sequence of the 12-residue epitope for the Ca²⁺-dependent monoclonal antibody, HPC4 (Figure 1). We then subcloned the modified factor X cDNA (hereafter called rfX) into *Hind*III and *Xba*I restriction enzymes sites of the pcDNA3.1 expression vector (Invitrogen, Carlsbad, CA) and expressed it in HEK293 cells as previously described (20). The fX mutants in the chymotrypsinogen numbering: Arg¹⁴³ → Ala (R143A), Lys¹⁴⁷ → Ala (K147A), Arg¹⁵⁰ → Ala (R150A), and Arg¹⁵⁴ → Ala (R154A), corresponding to residues Arg³⁶⁶, Lys³⁷⁰, Arg³⁷², and Arg³⁷⁶ in the fX cDNA numbering (29), were generated in the rfX cDNA by standard PCR mutagenesis methods as described (20). After confirmation of the accuracy of the mutagenesis by DNA sequencing, the constructs were introduced into HEK293 cells, and the mutant proteins were isolated from 20 L cell culture supernatants by a combination of immunoaffinity and ion exchange chromatography using the HPC4 monoclonal antibody (30) and a Mono Q FPLC column, respectively.

Human plasma proteins including factors Va, Xa, and X, prothrombin, and the factor X-activating enzyme from Russell's viper venom (RVV-X) were purchased from Haematologic Technologies Inc. (Essex Junction, VT). Tissue factor pathway inhibitor (TFPI) was from Monsanto Chemical Co. (St. Louis, MO). Human antithrombin and the active antithrombin-binding pentasaccharide fragment of heparin were generous gifts from Dr. Steven Olson (University of Illinois, Chicago). Phospholipid vesicles containing 80% phosphatidylcholine and 20% phosphatidylserine (PC/PS) were prepared as described (31). The chromogenic substrate Spectrozyme FXa (SpFXa) was purchased from American Diagnostica (Greenwich, CT), and S2238 was purchased from Kabi Pharmacia/Chromogenix (Franklin, OH). Prothrombin time (PT) reagent (Thrombomax with Ca²⁺), Polybrene, and unfractionated heparin were purchased from Sigma (St. Louis, MO). Normal pooled plasma and factor X deficient plasma from a genetically deficient patient were purchased from George King Bio-Medical, Inc. (Overland Park, KS).

Activation of Factor X Derivatives by RVV-X. Factor X derivatives were converted to active forms by RVV-X as described (32). Briefly, each factor X derivative (1 μ M) was incubated with RVV-X (20 nM) at 37 °C for 2 h in 0.1 M NaCl, 0.02 M Tris-HCl, pH 7.4, containing 0.1 mg/mL bovine serum albumin (BSA), 0.1% poly(ethylene glycol) 8000 (PEG 8000), and 2.5 mM Ca²⁺ (TBS + Ca²⁺). Time course analysis of the activation reactions indicated that all fX zymogens are converted to their active forms under these experimental conditions. Active-site concentrations of the recombinant factor Xa derivatives were determined by an amidolytic activity assay and titrations with human antithrombin assuming a 1:1 stoichiometry as described (20). These concentrations were within 80% of those expected based on zymogen concentrations as determined from the absorbance at 280 nm using the published absorption coefficient (33).

Cleavage of Chromogenic Substrates by the Factor Xa Derivatives. The steady-state kinetics of hydrolysis of SpFXa (7.8–1000 μ M) by the factor Xa derivatives (1 nM) were measured in TBS + Ca^{2+} at 405 nm at room temperature by a V_{max} Kinetic Microplate Reader (Molecular Devices, Menlo Park, CA) as described (20). The K_m and k_{cat} values for substrate hydrolysis were calculated from the Michaelis–Menten equation.

Activation of Prothrombin. The initial rate of prothrombin activation by the wild-type and mutant fXa derivatives was measured in both the absence and presence of factor Va as described (34). In the absence of the cofactor, the time course of activation was studied by incubating each fXa derivative (10 nM) with prothrombin (5 μ M) in TBS + Ca^{2+} at room temperature. At different time intervals, small aliquots of the activation reactions were transferred into wells of a 96-well assay plate containing S2238 (100 μ M in TBS containing 20 mM EDTA, and in 100 μ L final volume). The initial rate of activation was determined by measuring the increase in amidolytic activity of the samples toward S2238 as monitored at 405 nm by a V_{max} Kinetic Microplate Reader. The concentrations of thrombin generated in the activation reactions were determined from a standard curve prepared from the cleavage rate of S2238 by known concentrations of thrombin under exactly the same conditions.

In the presence of the cofactor, the affinity of fXa derivatives for binding factor Va was evaluated by a prothrombinase assay as described (34). Briefly, fXa (0.2 nM) was incubated with varying concentrations of human factor Va (0–50 nM) on 35 μ M PC/PS vesicles in TBS + Ca^{2+} at room temperature. The activation reaction was initiated with 1 μ M human prothrombin for 30 s, following which it was terminated by addition of EDTA to a final concentration of 20 mM. The concentrations of thrombin generated in the activation reactions were determined from a standard curve as described above. The concentration dependence of prothrombin activation in the presence of factor Va on PC/PS vesicles was also studied by a similar prothrombinase assay. In this case, factor Xa (20 pM) in complex with saturating factor Va (10 nM in all reactions) on PC/PS vesicles (35 μ M) was incubated with varying concentrations of human prothrombin (7.8–1000 nM) in TBS + Ca^{2+} . Following 15–60 s of incubation at room temperature, EDTA was added to a final concentration of 20 mM, and the concentrations of thrombin generated were determined by an amidolytic activity assay as described above. It was ensured that less than 15% of prothrombin was activated at all concentrations of the substrate.

Clotting Assays. The clotting activity of recombinant factor X was evaluated by a prothrombin time (PT) assay using a STart 4 fibrinometer (Diagnostica/Stago, Asnieres, France). Briefly, 0.1 mL of the PT reagent (Thrombomax with Ca^{2+}) was added to a mixture of 0.05 mL of the test sample (human plasma or recombinant fX) and 0.05 mL of fX-deficient plasma at 37 °C. Activities of the test samples were calculated from a standard curve made by using four different dilutions of normal pooled plasma ranging from 0.2 to 0.025 unit/mL (1 unit/mL corresponds to 8 μ g/mL fX). The clotting activities were calculated from at least four different dilutions that yielded clotting times in the linear range of the standard curve (17–35 s). A similar assay was used to evaluate the clotting activities of mutant fXa derivatives. In this case,

following activation by RVV-X and active-site titration, 0.1 mL of the PT reagent was added to a mixture of 0.05 mL of wild-type or mutant fXa (final concentrations of 31.25–250 pM) and 0.05 mL of fX-deficient plasma at 37 °C. The clotting activities of fXa derivatives were evaluated by comparing the linear range of log–log plots of clotting times (28–90 s) vs fXa concentrations.

Inactivation by Antithrombin. The rate of inactivation of the fXa derivatives by antithrombin in both the absence and presence of heparin cofactors was measured under pseudo-first-order rate conditions by a discontinuous assay as described (12). In the absence of a cofactor, 1 nM factor Xa was incubated with 125–1000 nM human antithrombin in TBS + Ca^{2+} at room temperature in 50 μ L volumes in 96-well polystyrene plates. In the presence of heparin cofactors, the reaction conditions were the same except that the rate of factor Xa inhibition (0.5 nM) was monitored at a fixed concentration of antithrombin (200 nM) and varying concentrations of cofactors (0.5–2 nM heparin, and 5–40 nM pentasaccharide). After a period of time (10 s to 40 min depending on the rate of the reactions), 50 μ L of SpFXa (500 μ M) in TBS containing 1 mg/mL Polybrene was added to each well, and the remaining enzyme activity was measured with a V_{max} Kinetics Microplate Reader. The observed pseudo-first-order rate constants (k_{obs}) were determined by fitting data to an exponential loss of activity with a zero endpoint. The second-order association rate constants for uncatalyzed and catalyzed reactions were obtained from the slopes of linear plots of k_{obs} vs the concentration of antithrombin or antithrombin–heparin complex, respectively, in accordance with eq 1, as described (12).

$$k_{\text{obs}} = k_{\text{uncat}} \times [\text{AT}]_{\text{free}} + k_{\text{Hep}} \times [\text{AT–Hep}] \quad (1)$$

In this equation, k_{uncat} and k_{Hep} are the second-order rate constants for uncatalyzed and heparin (or pentasaccharide)-catalyzed reactions, respectively, and $[\text{AT}]_{\text{free}}$ and $[\text{AT–Hep}]$ represent the free and antithrombin–heparin cofactor complex concentrations, which were calculated from the dissociation constants for the antithrombin–heparin cofactor interactions ($K_D = 5$ and 23 nM for heparin and pentasaccharide, respectively) and total concentrations of antithrombin and heparin cofactors using the quadratic equation as described (35).

Interaction with TFPI. The ability of the fXa derivatives to bind TFPI was evaluated by incubating fXa (0.3–1.0 nM) with different concentrations of TFPI (0.195–3.125 nM) in TBS + Ca^{2+} in 50 μ L volumes in 96-well polystyrene plates as described above for antithrombin. Following 30 min incubation at room temperature, 25 μ L of SpFXa was added to a final concentration of 200 μ M, and the K_i values were estimated by nonlinear regression analysis of data using eq 2, for tight binding inhibitors as described (36):

$$V_s/V_o = \{E_o - I_o - K_i + [(E_o + I_o + K_i)^2 - 4E_o \times I_o]^{1/2}\}/2E_o \quad (2)$$

where V_s and V_o are the steady-state velocities of chromogenic substrate hydrolysis in the presence and absence of TFPI, respectively, E_o and I_o are the total concentrations of fXa and TFPI, respectively, and K_i is the inhibition constant.

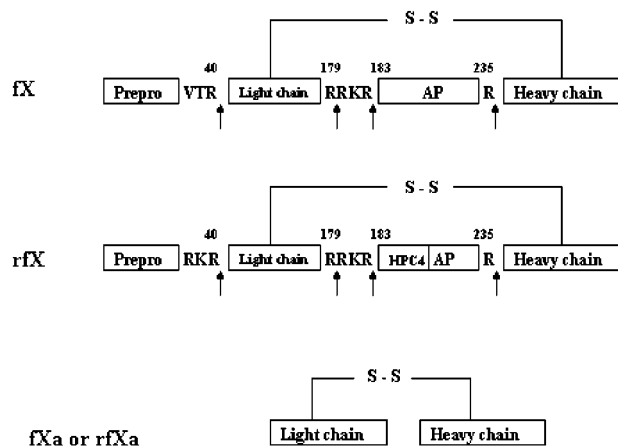


FIGURE 1: Schematic representations of modifications introduced into human factor X. The known cleavage sites on wild-type fX are indicated by arrows at the top figure. Cleavage at Arg⁴⁰ removes the leader prepropeptide (prepro) from the mature polypeptide. Processing at the RRKR sequence (residues 179–182) produces the native two-chain form circulating in plasma. Cleavage at Arg²³⁵ (Arg¹⁵ in chymotrypsinogen numbering) by RVV-X or physiological activators removes the activation peptide (AP) from the N-terminus of the heavy chain, leading to activation of fX. In the middle figure, rfX was modified to contain a tribasic processing site by replacing VT (residues 38 and 39) with RK, and the first 12 residues of the heavy chain on the activation peptide (residues 183–194) were replaced with the 12-residue epitope of the Ca²⁺-dependent monoclonal antibody, HPC4, as described under Materials and Methods. The bottom figure shows that cleavage of the activation peptide from either fX or rfX yields fXa molecules with identical structures. See ref (29) for fX numbering.

Data Analysis. The Enzfitter (R. J. Leatherbarrow, Elsevier, Biosoft) computer program was used to fit data to appropriate equations. All values are the average of at least three independent measurements \pm SE.

RESULTS

Expression and Purification of Factor X Derivatives. The wild-type and mutant factor X zymogens were expressed in a novel expression/purification vector system described under Materials and Methods. This vector system, which replaces the first 12 N-terminal residues of the activation peptide of fX with the epitope for the Ca²⁺-dependent monoclonal antibody HPC4 (Figure 1), has been extremely useful for efficient expression and easy purification of wild-type and mutant fX derivatives in 293 cells cultured in the presence of vitamin K. Following collection of a 20 L cell culture supernatant for each derivative, and its concentration by an Amicon concentrator equipped with S1Y10 spiral cartridge (Millipore, Beverly, MA), recombinant proteins were purified by immunoaffinity chromatography on an immobilized HPC4 monoclonal antibody column as described (30). Substitution of EDTA with Ca²⁺ in TBS was sufficient to elute recombinant fX derivatives from the HPC4 column. Further purification on an FPLC Mono Q column fractionated the HPC4 eluate into three distinct peaks eluting from the ion exchange column at \sim 0.2, \sim 0.3, and \sim 0.4 M NaCl (Figure 2A). SDS-PAGE and kinetic analysis suggested that the first peak had a lower relative molecular mass with no activity (data not shown). The second and third peaks of rfX exhibited similar molecular masses and comparable amidolytic activities; however, only the third peak had a clotting activity that was identical to that of plasma-derived fX, as

determined in a PT assay (Figure 2B). These results suggested that the second peak is a partially, and the third peak is a fully, γ -carboxylated protein. Consistent with this, rfXa exhibited essentially indistinguishable prothrombinase activity on PC/PS vesicles (see below). SDS-PAGE analysis of the third Mono Q peak of rfX derivatives suggested that the recombinant proteins are purified to homogeneity and that they all migrate with similar molecular masses as the plasma-derived fX (Figure 3). However, the R154A mutant appeared to migrate as a doublet. All derivatives could be converted to their active forms by RVV-X as determined by an amidolytic activity assay using SpFXa. Following complete activation, the concentrations of fXa derivatives were determined by an amidolytic activity assay and active-site titration with known concentrations of human antithrombin. These concentrations were within 70–100% of those expected based on zymogen concentrations as determined from the absorbance at 280 nm. The poorest correlation between the activities and zymogen concentrations based on the absorbance was observed for the R154A mutant (\sim 70%). Noting that this mutant also migrated as a doublet on SDS-PAGE, it is possible that mutagenesis of Arg¹⁵⁴ results in instability and possible cleavage of a short peptide from the mutant zymogen. The observation that the activity of the R154A fXa was also not stable is consistent with this possibility. Thus, all experiments with this mutant were conducted with freshly activated zymogen. As expected, since the activation peptide of the recombinant fX is cleaved off during its activation by RVV-X, the N-terminal HPC4 epitope is removed along with the activation peptide, and thus the activated form of the third peak has structure and activity identical to those of plasma-derived fXa (Figure 1).

Amidolytic Activity. The kinetic parameters for the hydrolysis of SpFXa by wild-type and recombinant fXa derivatives are presented in Table 1. All fXa derivatives cleaved the chromogenic substrate with similar K_m and k_{cat} values, suggesting that the mutagenesis did not adversely affect the folding and reactivity of the catalytic pocket.

Prothrombin Activation. The catalytic efficiency of fXa derivatives to activate prothrombin was studied in both the absence and presence of factor Va and Ca²⁺ on PC/PS vesicles (prothrombinase complex). The time course of activation in the absence of a cofactor indicated that all fXa derivatives activate prothrombin with similar catalytic efficiency (data not shown). A similar 0.33–0.37 nM/min thrombin was generated by both plasma-derived fXa and rfXa derivatives under the experimental conditions described under Materials and Methods (5 μ M prothrombin and 10 nM fXa). Similar to results obtained with the cleavage rate of SpFXa, these results suggested that the mutagenesis had no adverse effect on the folding of the recombinant proteins. Further support for this proposal is provided by the observation that fXa mutants interacted with factor Va with similar affinities of 1.5 nM as determined by a prothrombinase assay described under Materials and Methods. Detailed kinetic analysis further suggested that all fXa derivatives have a similar prothrombinase activity (k_{cat}/K_m) toward the activation of prothrombin, which suggests that the basic residues of the autolysis loop contribute minimally to the specificity of fXa interaction with either the cofactor or the substrate in the activation complex (Figure 4A, and Table 1). In agreement with this observation, the clotting activities of all factor Xa

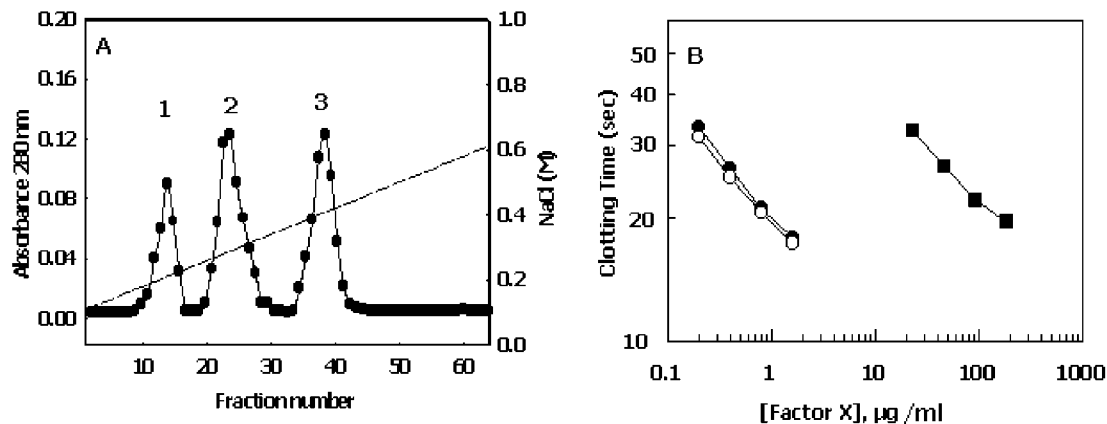


FIGURE 2: NaCl-gradient elution profile of the recombinant fX from the Mono Q ion exchange column (panel A) and comparison of its clotting activity with plasma fX (panel B). (A) HPC4 immunoaffinity-purified recombinant fX was applied on the Mono Q FPLC column and eluted with a linear gradient of 0.1–0.6 M NaCl as described under Materials and Methods. The bound proteins were eluted as three distinct peaks (1–3). Peak 1 migrated as a low molecular mass species (<20 kDa) with no amidolytic activity (data not shown). Peaks 2 and 3 had similar molecular masses and amidolytic activities (data not shown); however, only peak 3 had a normal clotting activity as shown in panel B. (B) The clotting activities of plasma fX (●) and recombinant fX derived from either peak 2 (■) or peak 3 (○) are determined at four different dilutions (0.2–1.6 μg/mL for both plasma and peak 3 fX; and 23–185 μg/mL for peak 2 fX) by a PT assay using factor X deficient plasma as derived under Materials and Methods. The clotting activities of plasma and recombinant fX from peak 3 are indistinguishable. The activity of fX from peak 2 is impaired more than 100-fold. A standard curve prepared from four different dilutions of normal pooled plasma (1/5, 1/10, 1/20, and 1/40) corresponding to 0.2–0.025 unit/mL fX (1 unit/mL corresponds to 8 μg/mL fX) gave clotting times (17–35 s) which were identical with those obtained for the plasma or recombinant fX (not shown).

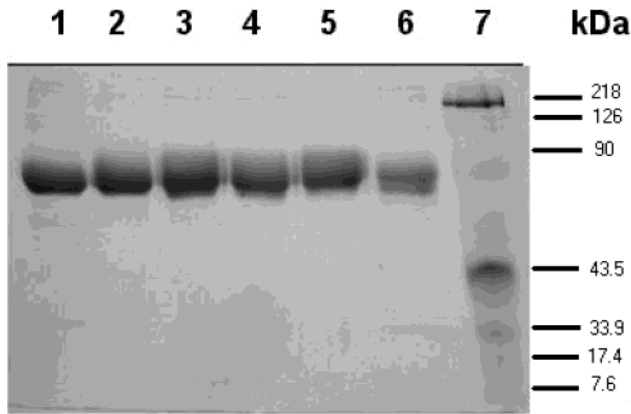


FIGURE 3: SDS–polyacrylamide gel analysis of the plasma-derived and recombinant fX derivatives under nonreducing conditions. Lane 1, plasma-derived human fX; lane 2, recombinant human fX; lane 3, R143A; lane 4, K147A; lane 5, R150A; lane 6, R154A; and lane 7, molecular mass standards in kDa.

derivatives were essentially mirror images of their prothrombinase activities in the purified system (Figure 4B).

Interaction with TFPI. K_i values for the binding of TFPI to fXa derivatives are presented in Table 1. All mutants interacted with TFPI with similar or at most ~2-fold impaired affinities, suggesting that the basic residues of the autolysis loop of fXa, with the exception of perhaps a minor contribution from the two residues Lys¹⁴⁷ and Arg¹⁵⁴, do not play a dominant role in tight binding of fXa to TFPI.

Reaction with Antithrombin. The reactivities of the fXa derivatives with antithrombin were examined in both the absence and presence of heparin cofactors. As shown in Figure 5A and Table 2, wild-type fXa and the R154A mutant reacted with antithrombin with similar rate constants in the absence of cofactors. However, there was a modest improvement (~2-fold) in the reactivities of the R143A and K147A mutants with the serpin, under the same conditions. These results suggest that the positive charges and/or the sizes of Arg¹⁴³ and Lys¹⁴⁷ may be inhibitory for interaction of fXa

Table 1: Kinetic Parameters for Wild-Type and Autolysis Loop Mutants of fXa in Hydrolysis of SpFXa, Activation of Prothrombin, and Interaction with TFPI^a

	SpFXa		prothrombin		TFPI
	K_m (μM)	k_{cat} (s ⁻¹)	K_m (nM)	k_{cat} (s ⁻¹)	K_i (nM)
pFXa	89.6 ± 3.9	125.7 ± 1.7	29.0 ± 3.0	26.5 ± 0.7	0.15 ± 0.02
rfXa	83.0 ± 3.9	126.5 ± 1.8	26.5 ± 2.5	23.0 ± 0.5	0.11 ± 0.03
R143A	67.5 ± 4.1	98.6 ± 1.7	18.7 ± 1.7	17.2 ± 0.3	0.14 ± 0.04
K147A	68.7 ± 3.3	115.2 ± 1.6	17.9 ± 1.4	19.0 ± 0.3	0.24 ± 0.06
R150A	64.9 ± 3.0	111.3 ± 1.4	25.4 ± 1.4	21.2 ± 0.3	0.09 ± 0.02
R154A	121.5 ± 6.4	130.6 ± 2.2	22.9 ± 2.2	16.9 ± 0.4	0.21 ± 0.04

^a The kinetic constants of fXa derivatives toward hydrolysis of SpFXa were determined by incubating each fXa derivative (1 nM) with increasing concentrations of the chromogenic substrate (7.8–1000 μM) in TBS + Ca²⁺ as described under Materials and Methods. The kinetic values for the prothrombin activation were determined by incubating each fXa derivative (20 pM) in complex with human factor Va (10 nM) on PC/PS vesicles (35 μM) with increasing concentrations of human prothrombin (7.8–1000 nM) in TBS + Ca²⁺. The values are derived from fitting of data to Michaelis–Menten equation. The K_i values for binding to TFPI were determined by incubating each fXa derivative (0.3–1.0 nM) with TFPI (0.195–3.125 nM) in the same buffer. Following 30 min of incubation at room temperature, SpFXa was added to a final concentration of 200 μM, and the K_i values were estimated by nonlinear regression analysis of data using eq 2 as described under Materials and Methods. The values are averages of three independent measurements ±SE.

with the native conformation of antithrombin, and thus their substitution with Ala alleviates these inhibitory interactions. A small, but reproducible extent of impairment (1.5-fold) in the reactivity of the R150A mutant was also observed with antithrombin in the absence of a cofactor. On the other hand, the reactivities of these mutants with the antithrombin–pentasaccharide complex were nearly normal for the R143A, K147A, and R154A mutants; however, the reactivity of the R150A mutant was impaired ~10-fold (Figure 5B, and Table 2). Further inhibition studies with the antithrombin–heparin complex indicated that the template effect of high molecular weight heparin in acceleration of the inhibition of R150A by antithrombin was not impaired (Table 2, the ratio of

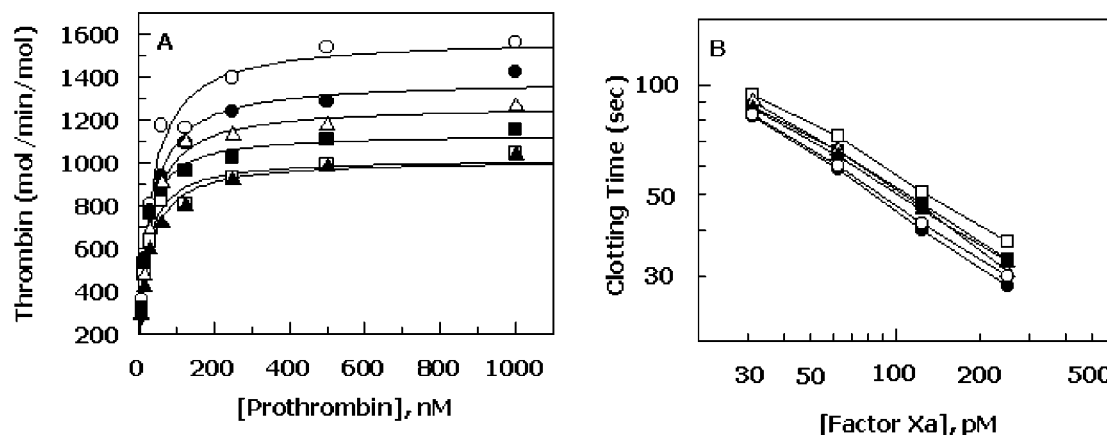


FIGURE 4: Comparisons of the catalytic properties of fXa derivatives in prothrombinase (panel A) and clotting assays (panel B). (A) The initial rate of activation of increasing concentrations of human prothrombin (7.8–1000 nM) by each fXa derivative (20 pM fXa) in complex with 10 nM human factor Va on 35 μ M PC/PS vesicles was measured in TBS + Ca^{2+} from the rate of thrombin generation as measured by an amidolytic activity assay using the chromogenic substrate S2238 as described under Materials and Methods. The solid lines are nonlinear regression fits of data to the Michaelis–Menten equation. (B) The clotting activities of the fXa derivatives (31.25–250 pM) were determined by a PT assay using fX-deficient plasma as described under Materials and Methods. The symbols in both panels are as follows: plasma-derived fXa (○); recombinant fXa (●); R143A (□); K147A (■); R150A (△); R154A (▲).

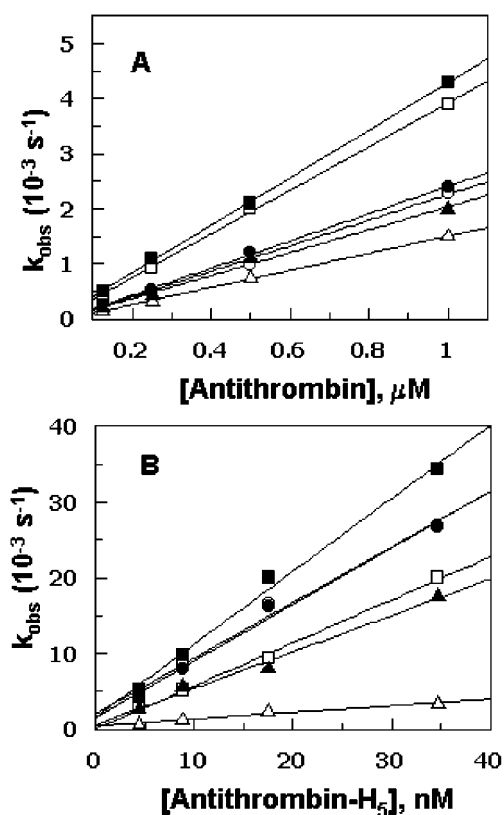


FIGURE 5: Dependence of observed pseudo-first-order rate constants (k_{obs}) on the concentration of antithrombin or antithrombin–pentasaccharide complex. (A) Each fXa derivative (1 nM) was incubated with human antithrombin (125–1000 nM) for 5–40 min at room temperature. The k_{obs} values were calculated and plotted against the concentrations of antithrombin as described under Materials and Methods. (B) The same as (A) except that the inhibition of 0.5 nM fXa was monitored with 200 nM antithrombin in complex with varying concentrations of pentasaccharide (5–40 nM). The k_{obs} values were plotted against the concentrations of the antithrombin–pentasaccharide complexes which were calculated based on their dissociation constant as described under Materials and Methods. The solid lines are computer fits of data to a linear equation. The symbols in both panels are as follows: plasma-derived fXa (○); recombinant fXa (●); R143A (□); K147A (■); R150A (△); R154A (▲).

heparin to pentasaccharide presented in the last column). These results suggest that Arg¹⁵⁰ makes a productive interaction specifically with the pentasaccharide-induced conformation of antithrombin, and thus its substitution with Ala leads to a significant impairment in the rate of mutant fXa inhibition by the activated conformation of the serpin.

It should be noted that similar to the reaction of antithrombin with wild-type fXa, inhibition stoichiometries of ~ 1 –1.5 (12, 21) were observed for all fXa derivatives in the presence of heparin, suggesting that mutagenesis of the autolysis loop does not influence the substrate pathway of the protease reaction with antithrombin.

DISCUSSION

In this study, we have substituted the basic residues, Arg¹⁴³, Lys¹⁴⁷, Arg¹⁵⁰, and Arg¹⁵⁴ of the autolysis loop of fXa with Ala using a novel expression/purification vector system and isolated fully γ -carboxylated proteins to homogeneity. Following activation by RVV-X, all mutant enzymes exhibited normal amidolytic activity toward hydrolysis of SpFXa, suggesting that the mutagenesis of the autolysis loop did not adversely affect the folding or the reactivity of the catalytic pocket of mutant enzymes. Further evidence for this was provided by the observation that all mutants had similar proteolytic activity toward activation of prothrombin in both the absence and presence of factor Va on PC/PS vesicles. Moreover, all mutants bound to factor Va with similar affinities of 1.5 nM as determined by a prothrombinase assay and exhibited similar activities as demonstrated by a clotting assay using fX-deficient plasma. Taken together, these results suggest that the mutants folded properly and that the basic residues of the autolysis loop do not noticeably contribute to the recognition specificity of fXa in the prothrombinase complex.

On the other hand, the basic residues of the autolysis loop may be more critical for interaction of fXa with the native and activated conformations of antithrombin. This is derived from the observation that the reactivities of both R143A and K147A with antithrombin in the absence of heparin cofactors were improved 2-fold, which suggests that both Arg¹⁴³ and

Table 2: Second-Order Inhibition Rate Constants (in $M^{-1} s^{-1}$) for Wild-Type and Autolysis Loop Mutants of fXa in Reaction with Antithrombin in the Absence and Presence of High Molecular Mass Heparin (Hep), and High-Affinity Pentasaccharide Fragment of Heparin (H_5)^a

	-cofactor $\times 10^3$	$H_5 \times 10^5$	$Hep \times 10^7$	fold catalytic effect		
				H_5	Hep	Hep/ H_5
pfXa	2.3 ± 0.1	7.3 ± 0.6	6.8 ± 0.4	317	29565	93
rfXa	2.4 ± 0.1	7.4 ± 0.5	7.1 ± 0.3	308	29583	96
R143A	4.0 ± 0.1	5.7 ± 0.2	3.9 ± 0.5	142	9750	69
K147A	4.3 ± 0.1	9.6 ± 0.5	5.6 ± 0.7	223	13023	58
R150A	1.6 ± 0.1	0.88 ± 0.12	1.8 ± 0.1	55	11250	204
R154A	2.1 ± 0.1	4.8 ± 0.4	3.8 ± 0.3	228	18095	79

^a The uncatalyzed inhibition rate constants were determined by incubating each fXa derivative (1 nM) with human antithrombin (125–1000 nM) in TBS + Ca^{2+} . The pentasaccharide (H_5) or high molecular mass heparin (Hep) catalyzed rate constants were determined by the same procedure except that each fXa derivative (0.5 nM) was incubated with antithrombin (200 nM) in complex with 5–40 nM pentasaccharide or 0.5–2 nM heparin in TBS + Ca^{2+} . Following incubation for 10 s to 40 min at room temperature, SpFXa was added, and the second-order rate constants were obtained from the slopes of linear plots of observed pseudo-first-order rate constants vs the concentrations of antithrombin or antithrombin–heparin cofactor complexes as described under Materials and Methods. All values are averages of three independent measurements \pm SE.

Lys¹⁴⁷ make inhibitory interactions by virtue of their charges and/or sizes with the native conformation of the serpin, and thus their neutralization and/or reduction of the size of their side chains by mutagenesis alleviates the inhibitory interactions. However, the reactivities of these mutants with antithrombin in the presence of pentasaccharide or high molecular weight heparin were similar to wild-type fXa, which suggests that these basic residues are not critical for interaction with the activated conformation of the serpin. On the other hand, the reactivity of the R150A mutant with antithrombin was impaired 1.5-fold ($2.4 \times 10^3 M^{-1} s^{-1}$ for rfXa and $1.6 \times 10^3 M^{-1} s^{-1}$ for R150A) in the absence and an order of magnitude in the presence of pentasaccharide (Table 2). These results suggest that Arg¹⁵⁰ makes productive interactions with both native and activated conformations of antithrombin. Based on such results, we hypothesize that Arg¹⁵⁰ interacts with a complementary site of antithrombin; however, this site does not have the right distance and/or conformation to interact effectively with fXa unless the serpin is activated by heparin cofactors, and thus its substitution with Ala leads to a minor, but reproducible defect in the absence and a much more significant defect in the presence of pentasaccharide. These results suggest that the several hundredfold greater rate of fXa inhibition by activated antithrombin may partially be mediated through interaction of the serpin with the autolysis loop of fXa. Thus, the rate acceleration may arise both from the relief of inhibitory interactions in the unactivated inhibitor and from establishing new interactions with the activated inhibitor. Assuming that these effects are additive, such interactions could potentially account for $2 \times 2 \times 8$ (relief of two inhibitory interactions and creation of one promoting interaction) or 32-fold of the total 200–300-fold rate enhancement observed with the pentasaccharide in the reaction. However, further studies are required to verify whether these effects can make additive contributions to the rate enhancement of fXa inhibition by the activated antithrombin.

The mechanism by which the heparin-activated conformation of antithrombin inhibits fXa with a markedly improved rate constant is not very well-known. The traditional view is that the reactive site loop of antithrombin, although it has an optimal recognition sequence for fXa, does not have a proper conformation for effective docking into the catalytic pocket of the protease (19, 37). Thus, the binding of a unique pentasaccharide fragment of heparin on a positively charged helix (D-helix) of antithrombin induces a conformational change in the reactive site loop of the serpin that facilitates its optimal recognition by fXa. Such an allosteric activation of the reactive site loop of the serpin is associated with a dramatic enhancement in the reactivity of the serpin with some proteases, like fXa (19, 21) and factor IXa (38), but has minimal effect in the reactivity of the serpin with certain other proteases such as thrombin (21). However, recently new data have been presented which suggest that a heparin-induced allosteric activation of the reactive site loop of antithrombin may in fact not play a decisive role in the interaction of the serpin with fXa. This has been derived from the observation that systematic mutagenesis of the P6–P3' residues of the reactive site loop of antithrombin have not lead to a noticeable difference in the allosteric rate enhancement of the fXa inhibition by mutant serpins in the presence of pentasaccharide (18). Our own previously published data are in agreement with this observation as the replacement of the P4–P4' residues of antithrombin with the identical sequences of either one of the two fXa recognition sites of prothrombin resulted in mutants which were allosterically activated toward reaction with fXa to a similar extent as the wild-type serpin (39). Relative to α_1 -antitrypsin, the reactive site loop of antithrombin has three additional residues, Arg³⁹⁹, Val⁴⁰⁰, and Thr⁴⁰¹, at the C-terminal P' end of the loop (40). Our previous mutagenesis data indicated that these residues may also not be targets for the allosteric activation and subsequent productive interaction of antithrombin with the protease since their deletion resulted in mutants that exhibited improved reactivities with fXa in the absence and comparable reactivities in the presence of the heparin cofactors (41). Taken together, these observations support the suggestion that the allosteric activation of antithrombin is independent of the sequence of the reactive site loop of the serpin (18). Such results have raised the possibility that allosteric activation of antithrombin may expose a secondary binding site “exosite” on the serpin, outside the P6–P3' reactive site loop sequence, that can constitute a recognition site for fXa (18). No exosite on antithrombin that may be critical for the binary serpin–protease interaction has been identified. It is worth, however, noting that results of recent crystal structure determination of a serpin–trypsin Michaelis complex suggest that certain residues of the reactive site loop of the serpin (perhaps P9 and P10) interact with the autolysis loop of trypsin (42). It is not known if such interactions can specifically contribute to cofactor-dependent interaction of antithrombin with fXa.

In addition to having an important role in interaction with antithrombin, previous structural and molecular modeling data have indicated that the autolysis loop of fXa may also play a critical role for interaction with other physiological or nonphysiological inhibitors of fXa including TFPI, tick anticoagulant peptide, and antistasin. Molecular modeling

data, based on the structure of the second Kunitz domain of TFPI in complex with trypsin, predict that the basic residues of the autolysis loop would come in close contact with an acidic patch of TFPI (43). The observation that the K_i values for the TFPI inhibition of Lys¹⁴⁷ and Arg¹⁵⁴ mutants were elevated ~2-fold (Table 1) is consistent with this hypothesis. However, noting the low K_i of the fXa–TFPI interaction, our results do not assign a dominant role for the autolysis loop in the high-affinity interaction of fXa with this inhibitor. In the crystal structure of bovine fXa in complex with tick anticoagulant peptide, the basic residues of the autolysis loop are involved in several electrostatic interactions, including salt-bridges and hydrogen bonds, with the inhibitor (44). Similarly, in the molecular model of the fXa–antistatin complex, several backbone carbonyl oxygen atoms of the inhibitor have been predicted to interact with the side-chain amino groups of Lys¹⁴⁷ (45). It is also known that the autolysis loop of certain other serine proteases is involved in interaction with inhibitors. For instance, in a previous mutagenesis study with thrombin, deletion of three residues, Glu¹⁴⁶, Thr¹⁴⁷, and Trp¹⁴⁸, from the autolysis loop rendered the mutant protease susceptible to inhibition by the Kunitz inhibitors, soybean trypsin inhibitor and bovine pancreatic trypsin inhibitor, BPTI (25). Moreover, in the crystal structure of the trypsin–BPTI complex, Tyr¹⁵¹ of the autolysis loop has been shown to make electrostatic and van der Waals interactions with Arg¹⁷ and Val³⁴ of the inhibitor (46). Thus, it appears that the interaction of the autolysis loop of serine proteases with their target inhibitors is required for an efficient regulation of the proteolytic activity of these proteases.

In summary, results of this study suggest that the basic residues of the autolysis loop play a dual role in the reaction of fXa with antithrombin. The basic residues Arg¹⁴³ and Lys¹⁴⁷ impede the efficient interaction of fXa with the native conformation of antithrombin by repulsive/steric interactions, and a role for heparin may be to bind, and relocate, the complementary inhibitory residues on the serpin by an allosteric mechanism. On the other hand, Arg¹⁵⁰ makes a productive interaction with antithrombin; however, the complementary site on the native serpin does not appear to have the right distance and/or conformation for interaction with fXa, and the allosteric activation of the serpin by pentasaccharide makes the putative recognition site available for interaction with the basic residue of the autolysis loop. Thus, a role for pentasaccharide in allosteric activation of antithrombin is to bring an as yet unidentified site on the surface of the serpin into the proper alignment for interaction with the autolysis loop of fXa. By such a mechanism, the cofactor not only overcomes the inhibitory interactions of the basic residues, Arg¹⁴³ and Lys¹⁴⁷, but also facilitates the productive interaction of Arg¹⁵⁰ with the serpin. It is worth noting that Arg¹⁵⁰ is also conserved in the autolysis loop of factor IXa whose reaction with antithrombin is also sensitive to the rate-accelerating effect of heparin by an allosteric mechanism (38), but not in thrombin which reacts similarly with both the native and activated conformations of the serpin (21). Further mutagenesis work is in progress to determine whether the homologous basic residue of factor IXa also plays a similar role in the protease reaction with antithrombin.

ACKNOWLEDGMENT

We thank Audrey Rezaie for proofreading of the manuscript.

REFERENCES

1. Davie, E. W., Fujikawa, K., and Kisiel, W. (1991) *Biochemistry* 30, 10363–10370.
2. Jackson, C. M., and Nemerson, Y. (1980) *Annu. Rev. Biochem.* 49, 765–811.
3. Rosing, J., Tans, G., Govers-Riemslog, J. W. P., Zwaal, R. F. A. Z., and Hemker, H. C. (1980) *J. Biol. Chem.* 255, 274–283.
4. Mann, K. G., Jenny, R. J., and Krishnaswamy, S. (1988) *Annu. Rev. Biochem.* 57, 915–956.
5. Furie, B., and Furie, B. C. (1988) *Cell* 53, 505–518.
6. Stenflo, J. (1991) *Blood* 78, 1637–1651.
7. Girard, T. J., Warren, L. A., Novotny, W. F., Likert, K. M., Brown, S. G., Miletich, J. P., and Broze, G. J., Jr. (1989) *Nature* 338, 518–520.
8. Broze, G. J., Jr., Girard, T. J., and Novotny, W. F. (1990) *Biochemistry* 29, 7539–7546.
9. Gettins, P. G. W., Patston, P. A., and Olson, S. T. (1996) in *Serpins: Structure, Function and Biology*, pp 33–63, R. G. Lands Co., Austin, TX.
10. Carrell, R. W., Evans, D. L., and Stein, P. E. (1991) *Nature* 353, 576–578.
11. Rosenberg, R. D., and de Agostini, A. I. (1991) *Adv. Exp. Med. Biol.* 313, 307–316.
12. Rezaie, A. R., and Olson, S. T. (2000) *Biochemistry* 39, 12083–12090.
13. Rezaie, A. R. (2000) *Trends Cardiovasc. Med.* 10, 333–338.
14. Mann, K. G., Nesheim, M. E., Church, W. R., Haley, P., and Krishnaswamy, S. (1990) *Blood* 76, 1–16.
15. Anderson, P. J., Nasset, A., Dharmawardana, K. R., and Bock, P. E. (2000) *J. Biol. Chem.* 275, 16435–16442.
16. Krishnaswamy, S., and Betz, A. (1997) *Biochemistry* 36, 12080–12086.
17. Betz, A., and Krishnaswamy, S. (1998) *J. Biol. Chem.* 273, 10709–10718.
18. Chuang, Y.-J., Swanson, R., Raja, S. M., and Olson, S. T. (2001) *J. Biol. Chem.* 276, 14961–14971.
19. Huntington, J. A., McCoy, A., Belzar, K. J., Pei, X. Y., Gettins, P. G. W., and Carrell, R. W. (2000) *J. Biol. Chem.* 275, 15377–15383.
20. Rezaie, A. R. (2000) *J. Biol. Chem.* 275, 3320–3327.
21. Olson, S. T., Björk, I., Sheffer, R., Craig, P. A., Shore, J. D., and Choay, J. (1992) *J. Biol. Chem.* 267, 12528–12538.
22. Padmanabhan, K., Padmanabhan, K. P., Tulinsky, A., Park, C. H., Bode, W., Huber, R., Blankenship, D. T., Cardin, A. D., and Kisiel, W. (1993) *J. Mol. Biol.* 232, 947–966.
23. Bode, W., Brandstetter, H., Mather, T., and Stubbs, M. T. (1997) *Thromb. Haemostasis* 78, 501–511.
24. Bode, W., Mayr, I., Baumann, U., Huber, R., Stone, S. R., and Hofsteenge, J. (1989) *EMBO J.* 8, 3467–3475.
25. Le Bonniec, B. F., Guinto, E. R., and Esmon, C. T. (1992) *J. Biol. Chem.* 267, 19341–19348.
26. Shen, L., Villoutreix, B. O., and Dahlbäck, B. (1999) *Thromb. Haemostasis* 82, 1078–1087.
27. Thomas, L., Cooper, A., Bussey, H., and Thomas, G. (1990) *J. Biol. Chem.* 265, 10821–10824.
28. Wolf, D. L., Sinha, U., Hancock, T. E., Lin, P., Messier, T. L., Esmon, C. T., and Church, W. R. (1991) *J. Biol. Chem.* 266, 13726–13730.
29. Leytus, S. P., Foster, D. C., Kurachi, K., and Davie, E. W. (1986) *Biochemistry* 25, 5098–5102.
30. Rezaie, A. R., and Esmon, C. T. (1992) *J. Biol. Chem.* 267, 26104–26109.
31. Smirnov, M. D., and Esmon, C. T. (1994) *J. Biol. Chem.* 269, 816–819.
32. Rezaie, A. R. (1996) *J. Biol. Chem.* 271, 23807–23814.
33. DiScipio, R. G., Hermodson, M. A., Yates, S. G., and Davie, E. W. (1977) *Biochemistry* 16, 698–707.

34. Rezaie, A. R., and He, X. (2000) *Biochemistry* 39, 1817–1825.
35. Olson, S. T., Bjork, I., and Shore, J. D. (1993) *Methods Enzymol.* 222, 525–560.
36. Lindhout, T., Willems, G., Blezer, R., and Hemker, C. (1994) *Biochem. J.* 297, 131–136.
37. Carrell, R. W., Skinner, R., Jin, L., and Abrahams, J. (1997) *Thromb. Haemostasis* 78, 516–519.
38. Wiebe, E., O'Brien, L., Stafford, A., Fredenburgh, J., and Weitz, J. (2001) *Thromb. Haemostasis (Suppl.)*, P2101.
39. Rezaie, A. R., and Yang, L. (2001) *Biochim. Biophys. Acta* 1528, 167–176.
40. Huber, R., and Carrell, R. W. (1989) *Biochemistry* 28, 8951–8966.
41. Rezaie, A. R. (2002) *J. Biol. Chem.* 277, 1235–1239.
42. Ye, S., Cech, A. L., Belmares, R., Bergstrom, R. C., Tong, Y., Corey, D. R., Kanost, M. R., and Goldsmith, E. J. (2001) *Nat. Struct. Biol.* 8, 979–983.
43. Burgering, M. J. M., Orbons, L. P. M., van der Doelen, A., Mulders, J., Theunissen, H. J. M., Grootenhuys, P. D. J., Bode, W., Huber, R., and Stubbs, M. T. (1997) *J. Mol. Biol.* 269, 395–407.
44. Wei, A., Alexander, R. S., Duke, J., Ross, H., Rosenfeld, S. A., and Chang, C.-H. (1998) *J. Mol. Biol.* 283, 147–154.
45. Lapatto, R., Krengel, U., Schreuder, H. A., Arkema, A., de Boer, B., Kalk, K. H., Hol, W. G. J., Grootenhuys, P. D. J., Mulders, J. W. M., Dijkema, R., Theunissen, H. J. M., and Dijkstra, B. W. (1997) *EMBO J.* 16, 5151–5161.
46. Huber, R., Kukla, D., Steigemann, W., Deisenhofer, J., and Jones, T. A. (1974) in *Bayer Symposium V on Proteinase Inhibitors* (Fritz, H., Tschesche, H., Greene, L. J., and Truscheit, E., Eds.) pp 497–512, Springer-Verlag, Berlin, Heidelberg, and New York.

BI0255367